EPJ Web of Conferences **37**, 05007 (2012)
DOI: 10.1051/epjconf/20123705007

Towards a Measurement of the $\omega\pi$ Transition Form Factor

Farha Anjum Khan[a] for the WASA-at-COSY Collaboration

Forschungszentrum Jülich

Abstract. Two sets of experiments have been performed with the WASA detector at COSY. The intention is to compare the quality of the data between the pd→^{3}He ω and pp→pp ω reactions, in the sense of a feasibility and background study for $\omega \to \pi^0 e^+ e^-$ decays. The aim of the physics program is to determine the transition form factor of the ω meson which does not agree with standard Vector Meson Dominance. As a first step towards the $\omega\pi$ transition form factor, we study the decay with a real photon, $\omega \to \pi^0\gamma$. The status of the analysis is presented.

1 Introduction

The meson electromagnetic transition form factor is one of the fundamental properties of hadrons and their interactions. In the investigation of the quark-gluon plasma and medium modifications of hadrons, the knowledge of the lepton pair mass spectra is essential. In the standard model, the anomalous magnetic moment has three contributions, $a_\mu = a_\mu^{QED} + a_\mu^{weak} + a_\mu^{hadronic}$. The precise knowledge of the transition form factors is mandatory for evaluating the hadronic contributions. High precision measurements are now possible and further theoretical investigations are being developed [1].

The meson transition form factor is accessible via Dalitz decays. In the Dalitz decay a meson decays into a pseudoscalar meson (π^0) or a single photon (γ) (depending upon if the meson is a vector or a pseudoscalar) and a virtual photon (γ^*) which then decays into a dilepton. The transition form factor is experimentally determined by comparing the measured transition probability and QED predicted transition probability see eq. 1. The form factor $F(q^2)$ describes the electromagnetic structure at the $\omega\pi$ transition and is a function of q^2, where q^2 is 4-momentum transfer of the dilepton. The q^2 dependency of the transition form factor is described in the Vector Meson Dominance (VMD) model. The virtual photon can interact with a hadron not only directly but also after a transition to a virtual vector meson state such as ρ,ω and ϕ, which has the same quantum number as the photon. This photon-hadron interaction is predominant thus, vector meson dominance. This process is pronounced with time-like ($q^2 > 0$) photons when the squared 4-momentum approaches the squared mass of the vector meson, $m_\gamma^* = \sqrt{q^2} = m_{\rho,\phi,\omega}$. This realization results in a strong resonance enhancement in the spectrum. Then, having "passed the resonance maximum" (at $q^2 > m^2_{\rho,\phi,\omega}$), the form factor begins to diminish. The form factor is parametrize by pole formula as $F(q^2) = \left[1 - q^2/m^2_{\rho,\phi,\omega}\right]^{-1}$.

$$\frac{d\Gamma}{dq^2} = \left[\frac{d\Gamma}{dq^2}\right]_{\mathrm{QED}} \left|F(q^2)\right|^2 \tag{1}$$

Our aim is to determine the electromagnetic transition form factor for $\omega \to \pi^0 e^+ e^-$. Here, the transition form factor does not agree with VMD predictions, whereas other meson decays like $\pi^0 \to \gamma e^+ e^-$ and $\eta \to \gamma l^+ l^-$ are in agreement [2]. Recently, the NA60 collaboration confirmed this disagreement

[a] e-mail: f.khan@fz-juelich.de

in heavy ion collision [3,4]. The theoretical calculations are able to describe the data but there is deviations for the masses above 0.58 GeV/c^2 [5–7]. It would be useful to have data for e^+e^- with WASA-at-COSY as a different experimental method using elementary reactions. Our apporach involves the full reconstruction of the final state (including the real photon) and gives access to the small virtual photon masses below the dimuon mass [8].

The WASA-at-COSY facility is a 4π detector system, designed for the study of the hadronic production and the decays of light mesons. The unique high density pellet target combined with high intensity beams provides high luminosities. Data have been acquired for the study of the decay $\omega \rightarrow \pi^0 e^+ e^-$ (branching ratio $(7.7\pm0.6)\times10^{-4}$) using two different production mechanisms. In order to plan a high-statistics experiment, the experimental approach will be developed using a 4 week pd$\rightarrow{}^3$Heω test experiment and a 1 week pp$\rightarrow$ppω pilot run. For the pd reaction data have been recorded at two beam energies, 1.5 GeV and 1.45 GeV for the systematic studies of the background. The cross-section for ω production in the pd reaction is much smaller (ca. 84 nb [9]) compared to the pp reaction at 2 GeV (ca. 5.7 μb[10]). However, the pp reaction has larger multipion production production rates, for example the production rate of pp $\rightarrow$pp$\pi^+\pi^-\pi^0$ is 30 times larger than $\omega \rightarrow \pi^+\pi^-\pi^0$ [11]. This background channel is significant for the $\pi^0 e^+ e^-$ decay. The pd reaction is used to train the analysis for further development for the pp reaction. In the following, we report on the analysis of the pd reaction. We select two channels $\omega \rightarrow \pi^0\pi^+\pi^-$ (branching ratio (98.2±0.7)%) and $\omega \rightarrow \pi^0\gamma$ (branching ratio (8.28±0.28)%) as reference channels.

2 Status of Data Analysis

^{3}He particles are identified in the forward detection system consisting of tracking detectors and layers of range hodoscopes. We are using a ΔE-E method, as shown in fig. 1. The black curve marks the selected events in the ^{3}He band. The decay products are detected in the central part of the detector. The central detector consists of a mini drift chamber operated in the field of a superconducting solenoid, a thin plastic scintillator barrel and an electromagnetic calorimeter. We start the analysis with the real photon case $\omega \rightarrow \pi^0\gamma$.

Tagging on ω meson: ω mesons are tagged via the missing mass deduced from the ^{3}He and initial state kinematics. The missing mass spectra for both beam energies are shown in fig. 1. The experimental data show a clear peak at $m_\omega = 0.782$ GeV/c^2. The smooth background consists mainly of multipion production as is indicated by Monte Carlo simulations for background channels not stemming from ω decays. In order to subtract the background a polynomial + Gaussian fit function has been used. After subtracting the background the number of ω mesons at 1.5 GeV and 1.45 GeV is 1.13×10^5 and 0.92×10^5, respectively. The reconstruction efficiency at this point is 82% which leads to a total 2.5×10^5 number of ω mesons.

Full reconstruction of the $\pi^0\gamma$ final state: For $\omega \rightarrow \pi^0\gamma \rightarrow \gamma\gamma\gamma$, the 3 final state photons are reconstructed in the electromagnetic calorimeter. A kinematic fit is not yet employed but the overall kinematics of the system is limited by imposing a generous constraint on the total missing energy and the magnitude of the total missing momentum.

In addition, the selected events are checked for a monochromatic photon. In the 2-body decay $\omega\pi^0(\rightarrow \gamma_1\gamma_2)\gamma$ the π^0 and the bachelor photon γ go back-to-back in the the rest frame of the ω meson. The π^0 and the γ have a definite energy and the same momentum magnitude. The π^0 boosts the 2 decaying photons γ_1 and γ_2 in the direction of its momentum. Therefore the opening angle between γ_1 and γ_2 ($\theta^{cm}_{\gamma_1\gamma_2}$) is limited. This can be seen in the left panel of fig. 2 where the photons from the $\pi^0\gamma$ events are correlated in the range indicated by the red lines. For further analysis events with this $\theta^{cm}_{\gamma_1\gamma_2}$ and E^{cm}_γ range are selected.

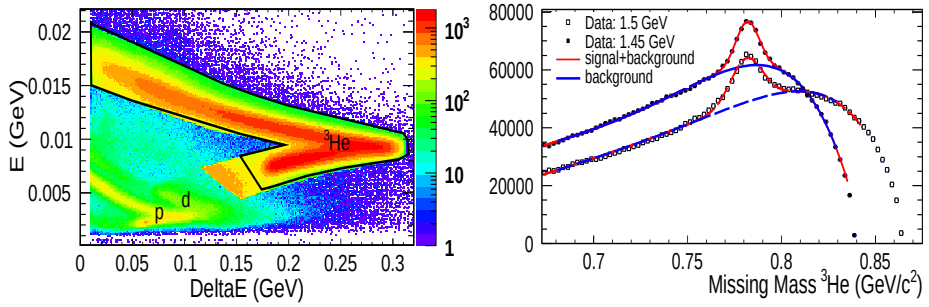

Fig. 1. Left: ΔE-E method for ^{3}He detection. The ^{3}He band is well separated. Right: missing mass distributions after ^{3}He selection for 1.5 GeV and 1.45 GeV beam energy. Both energies have a different phase space distribution and the same peak position.

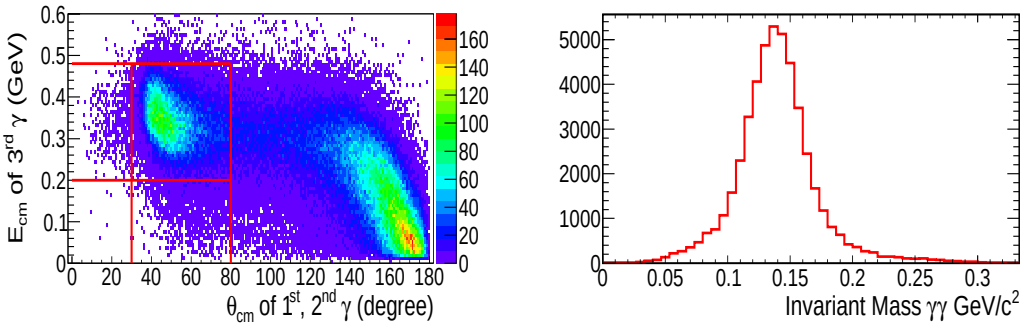

Fig. 2. The left panel shows the correlation between one photon energy and the opening angle of the two other photons for all combinations. Right panel: two-photon mass after the cut indicated in the left panel. A clean peak can be seen at the π^0 mass 0.135 GeV/c^2.

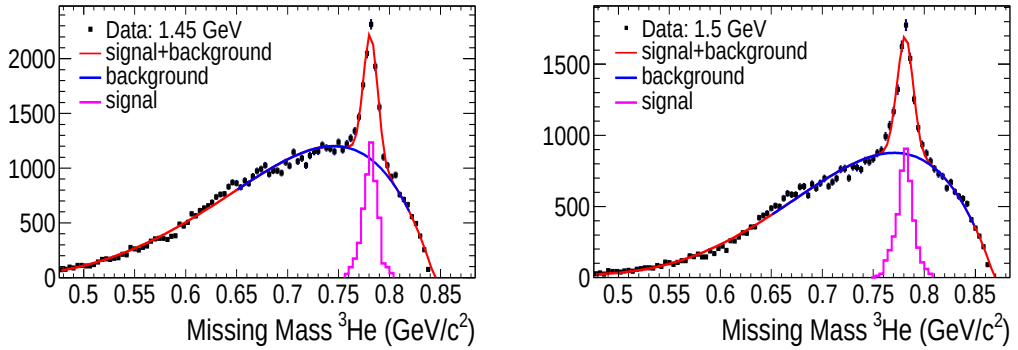

Fig. 3. The figures show the missing masses after ^{3}He selection and reconstruction of the $\pi^0\gamma$ final states for both beam energies. In both plots, the magenta histogram is the background subtracted ω peak.

After applying the above cuts on the decays kinematics, the invariant mass of $\gamma_1\gamma_2$ is shown in fig. 2. The reconstruction efficiency after the $\pi^0\gamma$ selection is 34%. The missing masses for both beam energies are shown in fig. 3 where the ω peak can be seen at m_ω = 0.782 GeV/c^2. Here, the background has been reduced compared to fig. 1 and the ω peak is more prominent. The background has been fitted using a polynomial function and has been subtracted from the experimental data. The total number of $\omega \rightarrow \pi^0\gamma$ events in the subtracted peaks (magenta curve) for both energies is (8700±156). Background events come from misidentified multipion contributions mainly $\pi^0\pi^0$ and $\pi^0\pi^0\pi^0$ and a

small contribution coming from other ω decays, as $\omega \to \pi^0\pi^+\pi^-$ and $\omega \to \pi^+\pi^-$ as indicated by Monte Carlo simulations.

3 Outlook

The next step is to fine tune the calibration and to do employ kinematic fitting in order to improve the events selection. For checking on the consistency of the analysis procedure a branching ratio cross check for $\pi^0\gamma$ will be done. The analysis of other reference channel $\omega \to \pi^0\pi^+\pi^-$ is going on. The analysis for the pd beamtime will be used to train the selection criteria, as a result the branching ratio measurement of $\omega \to \pi^0 e^+ e^-$ is the goal. This will be a first relevant result as the form factor has direct influence on the branching ratio. A complementary analysis of the pp pilot beam time is ongoing to make a strategy for the coming high statistics run for a precise determination of the transition form factor.

References

1. Editors: E. Czerwinski *et al.*, arXiv:1207.6556v1 [hep-ph], (2012).
2. L.G.Landsberg, Phys. Rept. **128**, (1985), 301.
3. An. Uras *et al.*, NA60 Collaboration, J. Phys. Conf. Ser. **128**, (2011), 012038.
4. R. Arnaldi *et al.*, NA60 Collaboration, Phys. Lett. B, **677**, (2009), 260.
5. C.Terschlüsen, *et al.*, Phys. Lett. B. **691**, (2010), 191.
6. C.Terschlüsen, *et al.*, arXiv:1204.4125v1 [hep-ph], (2012).
7. C.Terschlüsen, *et al.*, arXiv:1206.2253v1 [hep-ph], (2012).
8. H. H. Adam, *et al.*, WASA-at-COSY Collaboration, arxiv:nucl-ex/0411038.
9. K. Schonning, *et al.*, WASA-at-COSY Collaboration, Phys. Rev. C. **677**, (2009), 260.
10. S. Barsov, *et al.*, WASA-at-COSY Collaboration, Eur. Phys. J. A. **31**, (2007), 95.
11. C. Pauly *et al.*, CELSIUS-WASA Collaboration, Phys. Lett B,**649**, (2007), 122.